Journal of Alloys and Compounds 368 (2004) 260–268

Journal of ALLOYS AND COMPOUNDS

www.elsevier.com/locate/jallcom

Hydrogen induced structural and magnetic transformations in the hexagonal Laves phase $ErMn_2$

H. Figiel [a,*], A. Budziak [a], P. Zachariasz [a], J. Żukrowski [a], G. Fischer [b], E. Dormann [b]

[a] *Faculty of Physics and Nuclear Techniques, AGH University of Science and Technology, Pl-30-059 Kraków, Poland*
[b] *Physikalisches Institut, Universität Karlsruhe (TH), D-76128 Karlsruhe, Germany*

Received 14 August 2003; accepted 29 August 2003

Abstract

Powder samples of hexagonal Laves phase $ErMn_2H_x$ hydrides, with $0 < x \leq 4.3$, are characterised by X-ray analysis and SQUID magnetometry for temperatures ranging between 2 and 375 K. Structural transformations as function of the hydrogen concentration and temperature were observed. In particular, a decomposition of spinodal type has been found. It has been shown that structural transformations are reflected in the magnetic behaviour and that an increase of the Mn–Mn distance above the critical distance causes appearance of Mn magnetic moments. The analysis of the magnetic data as function of the hydrogen content, temperature and magnetic field shows that the Mn magnetic moments are antiferromagnetically coupled. The behaviour of these hydrides is compared with the properties of cubic hydrides.

Keywords: Rare earth compounds; Hydrogen absorbing materials; Crystal structure; X-ray diffraction; Magnetic measurements

1. Introduction

Hydrogen, which easily penetrates the rare earth metals and their compounds with 3d metals, causes many changes of their physical properties. Recently, very interesting transformations induced by hydrogen were observed in the cubic C15 (*Fd*3*m* space group) Laves phase type compounds of yttrium and rare earths with manganese, namely YMn_2H_x [1], $DyMn_2H_x$ [2], $TbMn_2H_x$ [3] and $GdMn_2H_x$ [4]. Hydrogen atoms are located there in the A2B2 interstitial sites. For intermediate hydrogen concentrations due to hydrogen atom interactions and diffusion, many unexpected structural and magnetic transformations take place in dependence on temperature and hydrogen concentration. In particular, temperature and hydrogen concentration dependent decomposition of spinodal type and increase of magnetic ordering temperatures above 200 K are observed. For the hydrides with the maximal hydrogen content ($x \cong 4.3$ per formula unit), the cubic or tetragonally distorted cubic structure is observed and the magnetic structure of antiferromagnetic type with ordering temperature above 300 K [5] appears. The crystal and magnetic structures are not affected by temperature for this hydrogen concentration. However, for the hydrides based on the hexagonal Laves phase (C14) only few reports on the structural [6] and NMR analysis [7] of the $SmMn_2H_2$ compound have been presented. Thus, in this work we report our research of structural and magnetic properties for the hydrides of the hexagonal phase $ErMn_2$. This system also easily absorbs hydrogen, and the aim of this work is to present and discuss the hydrogen induced structural and magnetic changes in this compound.

The $ErMn_2$ compound that crystallises as the hexagonal C14 type Laves phase ($P6_3/mmc$ space group), orders magnetically at 15 K [8,9]. In this compound, no magneto-volume effect appears, because the magnetic ordering is related with coupling between magnetic moments of erbium, and no magnetic moments of manganese exist due to an Mn–Mn distance smaller than the critical value [10].

2. Experimental

2.1. Sample preparation

The samples were prepared of high purity materials using the standard induction melting technique and then annealed

* Corresponding author. Tel.: +48-12-617-2554; fax: +48-12-634-1247.
E-mail address: figiel@uci.agh.edu.pl (H. Figiel).

0925-8388/$ – see front matter © 2003 Elsevier B.V. All rights reserved.
doi:10.1016/j.jallcom.2003.08.081

to obtain a well-defined single-phase material. Before hydriding the material was checked by X-ray diffraction. The hydriding was made using the standard technique described, e.g. in [1]. To achieve phase equilibrium, all the samples were annealed at 180 °C for a few hours. The samples of $ErMn_2H_x$ with hydrogen concentrations $x = 0$; 1.0; 2.0; 3.0; 3.5 and 4.3 were prepared.

2.2. X-ray measurements

The temperature dependent X-ray measurements were performed on a SIEMENS D5000 diffractometer using Cu K_α radiation ($\lambda = 1.54056$ Å) with continuous flow cryostat supplied by Oxford Instruments. The measurements were performed in the process of heating and at each temperature point the temperature was stabilised for about 40 min in order to reach the thermal phase equilibrium. To analyse and fit the spectra, the FULLPROF [11] program based on the Rietveld method was used. The measurements were made in the 68–375 K temperature range.

2.3. Magnetisation measurements

The magnetisation measurements were made using the Quantum Design MPMS SQUID magnetometer in the temperature range 2–375 K in external fields 0.1 and 50 kOe for increasing temperature. The process of cooling down was performed within 1–2 h. For the sample $ErMn_2H_{4.3}$, the susceptibility was measured both for cooling and heating.

To characterise the magnetic behaviour of the investigated $ErMn_2H_x$ hydrides above the ordering temperature in the paramagnetic phase, the temperature dependence of the susceptibility was analysed using the formula:

$$\chi(T) = \chi_{\text{dia}} + \frac{C}{(T - \Theta)} \quad (1)$$

with $\chi_{\text{dia}} = -1.6 \times 10^{-7}$ cm^3/g estimated from tabulated data [12]. In the magnetically ordered phase at 6 K, the field dependence of the magnetisation, M(H), was analysed in a slow ±55 kOe field cycle.

3. Experimental results

3.1. Structural measurements

The $ErMn_2$ starting material used for hydriding was checked by X-ray diffraction. The diffraction pattern of the $ErMn_2$ at RT proved its well defined C14 hexagonal structure and no impurities were visible in the pattern. Its lattice parameters are in agreement with the literature data [13]. In the investigated hydrides, there were detected some traces of Er_6Mn_{23} hydrides or oxides. At temperatures above 345 K, all the samples with x<4.3 were single hexagonal phase. For the samples with $x = 1$ (Fig. 1) and $x = 3$, the splits into two hexagonal phases as a function of temperature were observed. The samples with $x = 2$ and 3.5 remained single phase in the whole temperature range, but with some structural distortions. For $x = 4.3$, we observed the coexistence of two hexagonal phases up to 375 K. Measurements at temperatures above 375 K were not possible, because heating of the hydrides to higher temperatures leads

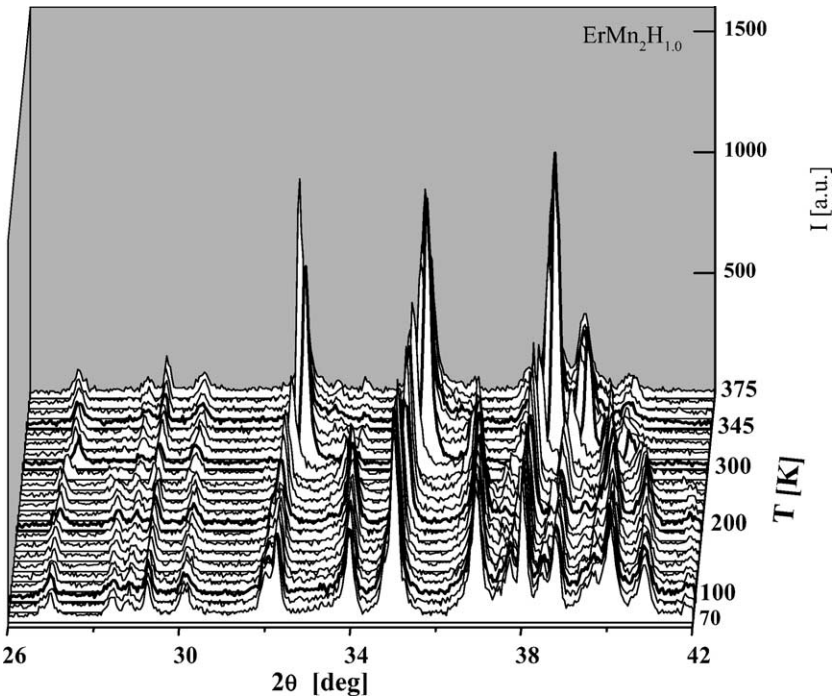

Fig. 1. The temperature evolution of the diffraction lines for $ErMn_2H_1$.

Table 1
Structural details of $ErMn_2H_x$ hydrides

Hydrogen content x	Structure at 350 K	Lattice parameters (Å)	Structure at 70 K	Unit cell parameters (Å, °)	
0.0	C14	$a = 5.29416$ $c = 8.64435$	C14	$a = 5.25476$ $c = 8.59381$	
1.0	C14—2 phases	$a_1 = 5.50707$ $c_1 = 8.99723$ $a_2 = 5.34094$ $c_2 = 8.71828$	C14—2 phases	$a_1 = 5.53197$ $c_1 = 9.06133$ $a_2 = 5.26279$ $c_2 = 8.59951$	
2.0	C14	$a = 5.56787$ $c = 9.07088$	$P1$	$a = 5.56513$ $b = 5.58443$ $c = 9.07567$	$\alpha = 89.97$ $\beta = 90.60$ $\gamma = 120.02$
3.0	C14	$a = 5.62604$ $c = 9.16138$	C14—2 phases	$a_1 = 5.62067$ $c_1 = 9.04039$ $a_2 = 5.67614$ $c_2 = 9.16924$	
3.5	C14	$a = 5.65726$ $c = 9.31407$	$P2_1/m$	$a = 5.64343$ $b = 5.69118$ $c = 9.29648$	$\alpha = \beta = 90$ $\gamma = 120.18$
4.3	C14—2 phases	$a_1 = 5.79874$ $c_1 = 9.55117$ $a_2 = 5.68132$ $c_2 = 9.43366$	C14—2 phases	$a_1 = 5.81318$ $c_1 = 9.53553$ $a_2 = 5.66804$ $c_2 = 9.43555$	

to hydrogen escape from the sample causing a decrease of the hydrogen content.

The structure details and the lattice parameters as obtained at 350 and 70 K are collected in Table 1. The temperature dependencies of the unit cell volume calculated using the parameters obtained from the FULLPROF refinements of the diffraction patterns for the investigated hydrides are presented in Fig. 2.

3.1.1. The $x \leq 2$ range

The most typical behaviour for this range of hydrogen concentration can be observed for the $ErMn_2H_1$ hydride. Below 345 K, the split of every structural line is observed (Fig. 1). This split can be related with the decomposition into two hexagonal phases: β_o close to the $ErMn_2$ with a very small amount of hydrogen ($x_0 \cong 0.01$) and β_r close to $ErMn_2H_2$ (Fig. 2). Taking into account the unit cell volume

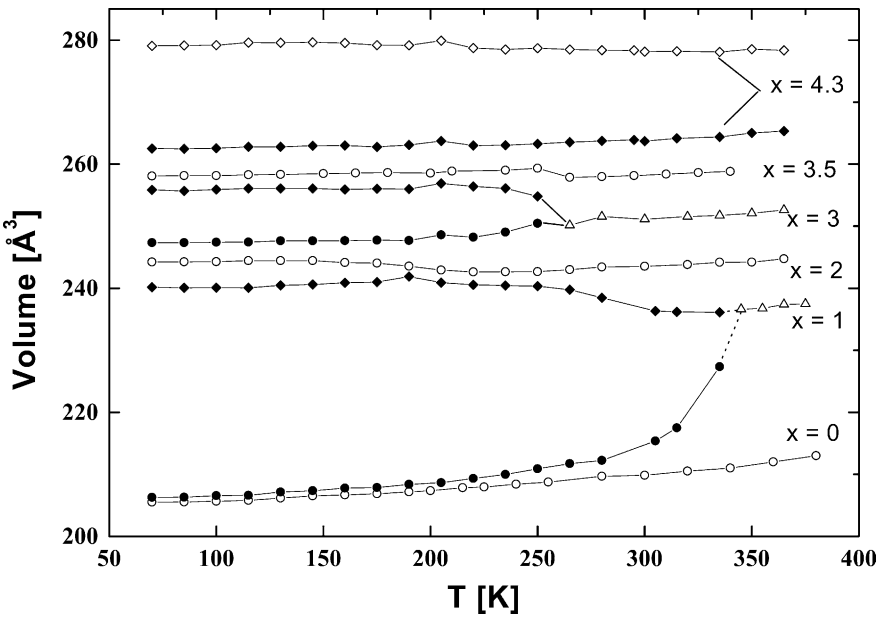

Fig. 2. The unit cell volume of $ErMn_2H_x$ hydrides in function of temperature.

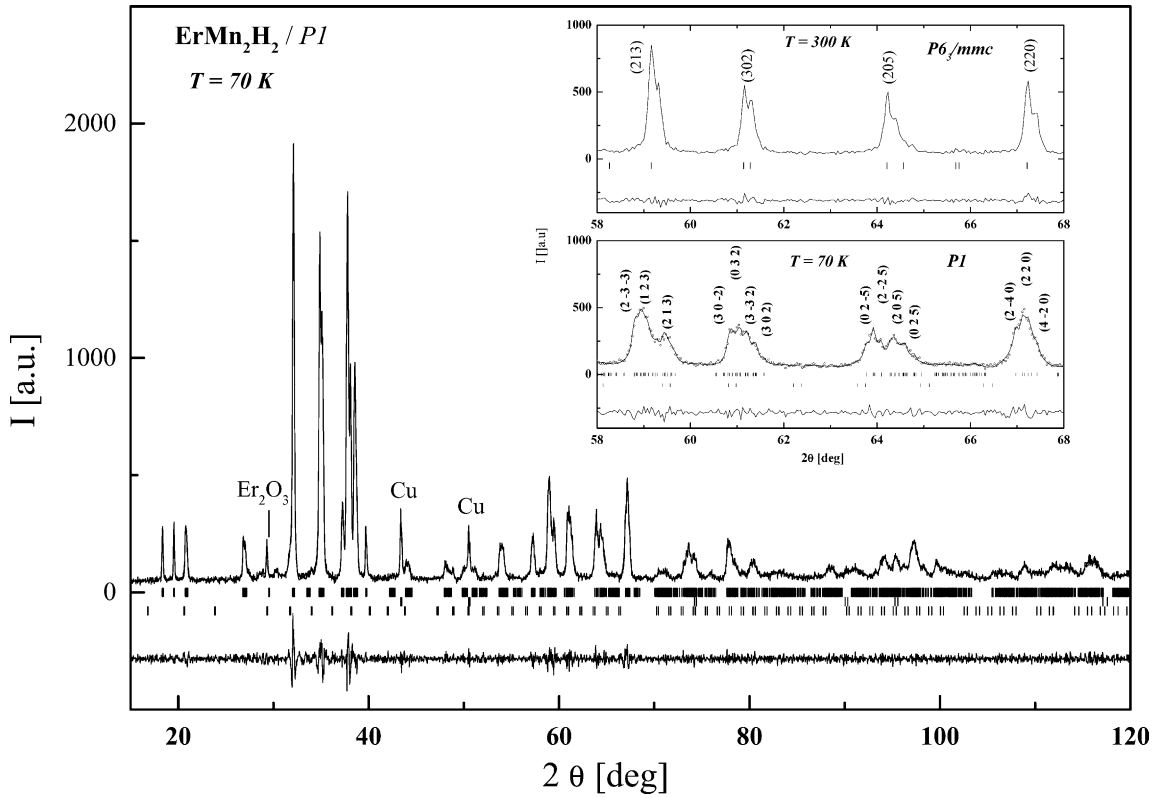

Fig. 3. The diffraction pattern for $ErMn_2H_2$ taken at 70 K with the fit to *P*1 structure. The Cu lines come from a sample container. The insert shows details of patterns ($2\Theta = 56$–66°) taken at 300 K (hexagonal structure) and at 70 K (*P*1 distorted structure).

gives $x_r \cong 1.8$ for β_r phase. The observed splitting can be understood as the decomposition of spinodal type. This behaviour is analogous to already observed decompositions in the cubic hydride $TbMn_2H_x$ [3] and $GdMn_2H_x$ [4]. However, for $ErMn_2H_1$ it appears at a temperature about 70 K higher than, e.g. the similar decomposition in $TbMn_2H_1$ hydride. Because it takes place at relatively high temperature (above RT), it means that the free energy difference between decomposed and uniform states must be very distinct.

The temperature behaviour of the $ErMn_2H_2$ hydride, for which we observe a triclinic distortion (*P*1) which appears at ~210 K is also very interesting. The optimal refinement for *P*1 triclinic structure close to C14 hexagonal structure for the diffraction pattern taken at 70 K is presented in Fig. 3. The insert in the Fig. 2 presents details of the patterns of $ErMn_2H_2$ for the characteristic range ($2\Theta = 56^\circ$–66°) taken at 70 and 300 K. The line shapes prove the appearance of distortion at 70 K. As visible the structure of the low angle lines at 70 K is very well reproduced for the proposed refinement with *P*1 type distortion. The attempts to refine the spectra with the structures of higher symmetry did not give satisfactory results. The temperature changes of the unit cell parameters obtained for *P*1 structure are presented in Fig. 4. The *P*1 type distortion is very small and the difference of lattice parameters $a_t - b_t$ reaches 0.02 Å (~0.3%), the difference of angles $(\beta_t - \alpha_t) \sim 0.6^\circ$ (~0.6%) and the relative change of angle γ_t is smaller than 0.07°. This behaviour is different from the previously reported spinodal decomposition of the analogous hexagonal $SmMn_2H_2$ hydride [14]. This proves that the type of rare earth atom influences the hydrogen induced phase transformations. This distortion can be also related with the onset of magnetic order, what will be discussed within the analysis of magnetic properties.

3.1.2. *The* $2 < x \leq 4.3$ *range*

From the fitting of the $ErMn_2H_3$ diffraction pattern, the spinodal type decomposition was found at temperature below 260 K (Fig. 2). This is decomposition into two hexagonal phases (β_{1m} and β_{2m}) with hydrogen content $x_{1m} \sim 2.53$ and $x_{2m} \sim 3.41$. It is worth noting here that the behaviour of $ErMn_2H_3$ is similar (split into two phases with small difference of hydrogen content) to that observed for $SmMn_2H_2$ [7]. The β_{1m} phase has lattice parameters closer to the β_r phase related to $ErMn_2H_2$. Also at ~210 K, some traces of its distortion can be detected in the diffraction pattern, however, not allowing for the proper fitting. The phase with x_{2m} possesses the volume that is close to that of $ErMn_2H_{3.5}$. The onset of this split coincides well with the step increase of the volume for the $ErMn_2H_{3.5}$ sample at ~260 K. The $ErMn_2H_{3.5}$ sample undergoes the distortion into $P2_1/m$ structure that starts at ~260 K, which is illustrated in Fig. 5. The distortion differs from that for $ErMn_2H_2$, because here the structure of higher symmetry is reached.

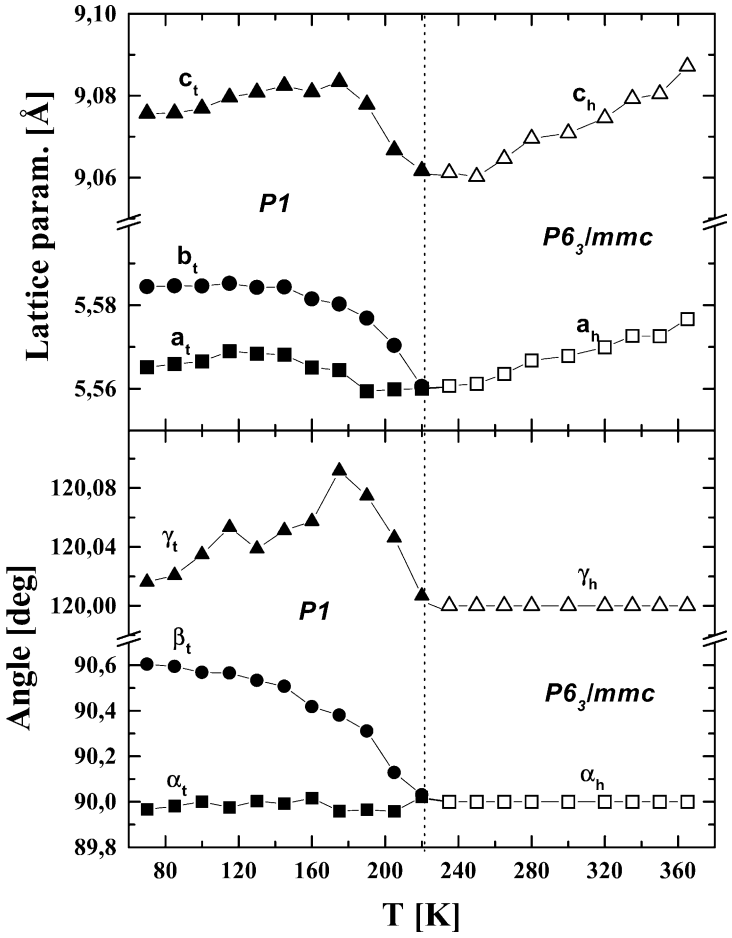

Fig. 4. The unit cell parameters for $ErMn_2H_2$ in function of temperature: (a) *a*, *b* and *c* parameters, (b) the angles as defined for a triclinic distortion.

The difference of lattice parameters $a_m - b_m$ amounts to 0.05 Å which gives ∼0.9%, much more than for $ErMn_2H_2$. The angles β_m and α_m do not change, and the relative change of γ_m is much bigger (∼0.2%) than for $ErMn_2H_2$. Presumably this difference reflects the role of hydrogen density in determining the final structure of the hydrides.

The $ErMn_2H_{4.3}$ sample consists of two hexagonal phases (β_{1h} and β_{2h}) with hydrogen concentrations $x_{1h} \sim 3.9$ and $x_{1h} \sim 4.8$ in the whole temperature range. The longer heat treatment does not lead to uniform distribution of hydrogen and reaching the single phase state. Perhaps it could be achieved at some temperature above 375 K, but as we have already mentioned at such temperature hydride becomes unstable because hydrogen can escape from the sample. Presumably, the lower volume phase β_{1h} is similar to that with $x = 3.5$, but because of the overlap of the lines of β_{1h} and β_{2h} phases in the diffraction pattern we were not able to fit this phase as distorted below 260 K. This result is in agreement with the existence of single phase hydrides for $x = 4.6$ and for $x = 4$ reported in [15]. The existence of such two phases is also similar to those observed for the cubic hydrides for $x \sim 4$ and can be related with hydrogen atoms entering the AB3 type interstitial sites.

4. Results of the magnetic measurements

The analysis of the magnetic data as a function of temperature and magnetic field shows that the details of the canted or collinear antiferromagnetic ordering of $ErMn_2H_x$ compounds are strongly influenced by the sign and strength of the interactions of the Mn and Er magnetic moments. Due to the analogy with the analysis and results of our earlier studies of $GdMn_2H_x$ [4] and $TbMn_2H_x$ [3], we confine this section to a summarising discussion based on Table 2 and Figs. 6–9.

The magnetic analysis supports the quality of the $ErMn_2$ starting material, allows an estimate of 2.5% for the presence of the Er_6Mn_{23} impurity phase and sets a corresponding upper limit for related hydrides. From the analysis of the susceptibility data for temperatures above the magnetic ordering temperature we estimated the μ_{eff} and Θ values given in Table 2. The values of Θ obtained from the low and high field data are different due to the influence of the mentioned magnetic impurity phases. For clarity, the temperature ranges used for the fit to Eq. (1) are given as well.

The structural transformations discussed above are clearly reflected in the magnetic behaviour. The temperature

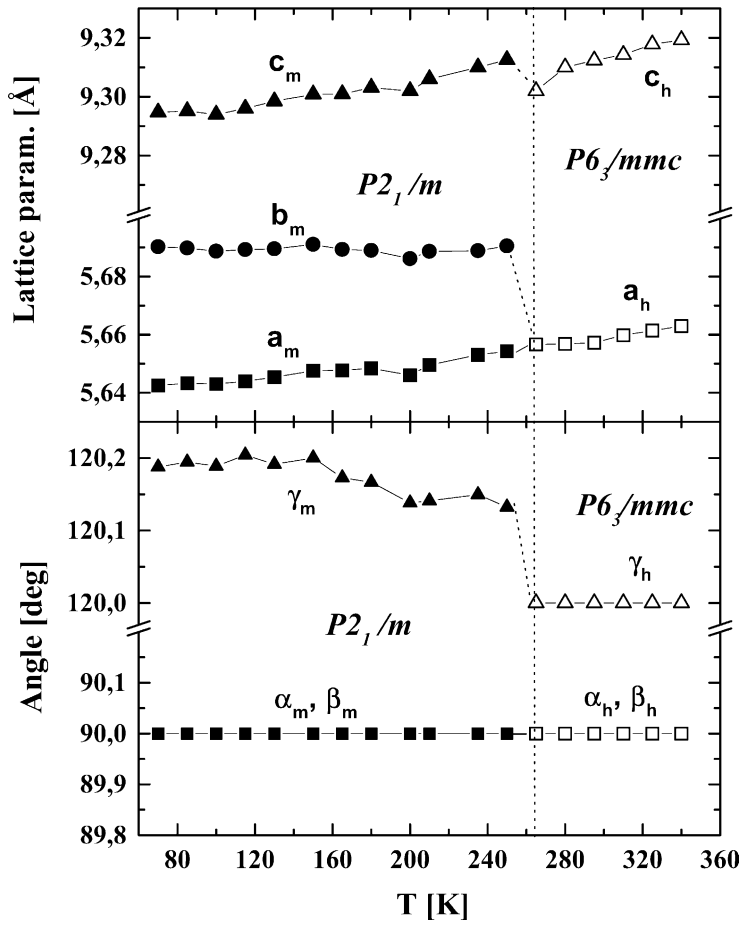

Fig. 5. The unit cell parameters for $ErMn_2H_{3.5}$ in function of temperature: (a) *a*, *b* and *c* parameters, (b) the angles as defined for a triclinic distortion.

dependence of the magnetic moment per gram of the respective samples observed at 0.1 kOe are presented in Fig. 6 (with different vertical scales for clarity), and the high field magnetisation curves are shown in Fig. 7. The total field-parallel magnetic moments μ_t per formula unit are indicated on the right hand scale of Figs. 6 and 7, thus simplifying a comparison with the saturation moment of 9 μ_B expected for the free ion Er^{3+} alone. The $ErMn_2$ data agree with earlier published results [9]. Apparently, in all samples except $ErMn_2$ the total moment is severely reduced compared to this limiting value due to non-parallel orientation of the Er moments or by the subtracted contribution of the Mn moments stabilized in the hydrides. In dependence on the hydrogen concentration, the magnetic anomalies observed at temperatures $T_{N,C} = 215$ K ($x = 1.0$), 205 K ($x = 2.0$) and 259 K ($x = 3.5$) are related with the onset of magnetic order which gets support from neutron diffraction study for $x = 2$ [16]. The shape of the magnetisation curves for $x = 1$ reflects the coexistence of $ErMn_2$ and hydrogen rich phases as deduced from the structural data. The magnetic ordering temperature ($T_{N,C}$) about 215 K comes from the hydrogen rich phase.

A ferrimagnetic canted magnetic structure of the $ErMn_2H_x$ hydrides can be deduced from the observed low magnetisation, and its changes with temperature can be

Table 2
Magnetic parameters of $ErMn_2H_x$ hydrides

x	μ_{eff} (μ_B/f.u.) 100 Oe	θ (K)	Temperature range (K)	μ_{eff} (μ_B/f.u.) 50 kOe	θ (K)	Temperature range (K)	$T_{N,C}$ (K)	T_M (K)
0.0	10.0 ± 0.5	11 ± 2	30–55	9.0 ± 0.3	18.5 ± 2	330–370	16 ± 1	175 ± 5, 330 ± 5
1.0	11.8 ± 2.0	−40 ± 20	335–370	9.5 ± 0.3	12 ± 6	330–370	16 ± 2, 215 ± 3	325 ± 5
2.0	10.0 ± 0.3	−31 ± 6	220–370	9.6 ± 0.3	1 ± 2	220–370	205 ± 5	–
3.5	–	–	–	10.0 ± 0.3	−18 ± 2	270–370	259 ± 5	25 ± 20, 120 ± 10
4.3	–	–	–	10.8 ± 1.0	−48 ± 6	320–370	315 ± 10	175 ± 5, 230 ± 5

T_M: temperature of additional magnetic anomalies.

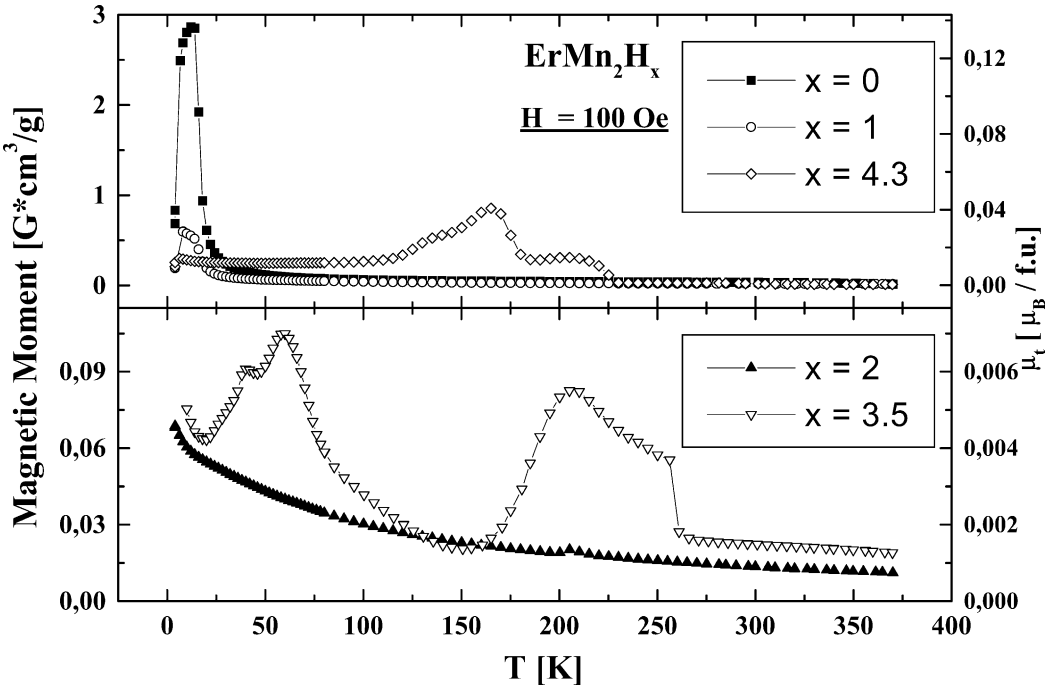

Fig. 6. The low field magnetisation in function of temperature for $ErMn_2H_x$ hydrides (100 Oe).

understood as related with varied interactions between the Er and Mn sublattices. The most collinear antiferromagnetic structure seems to be realized for $x = 2$. Actually, for x between 2 and 4.3, the magnetization does not reach saturation in maximal accessible field of 55 kOe (Fig. 8), which suggests a very strong antiferromagnetic coupling.

In the low field, magnetic moment data for $x = 3.5$ (Fig. 6) a step-like anomaly is visible exactly at the temperature (260 K) of the onset of the structural distortion (Fig. 5). The broad minimum of the susceptibility in the range 100–170 K corresponds to the temperature dependent changes of the distortion angles. Such correlation proves, that a non-collinear ferrimagnetic canted magnetic structure is formed for this hydride and that it is modified with temperature.

For $x = 4.3$, magnetic ordering for the phase with higher hydrogen content (β_{2h}) takes place presumably above

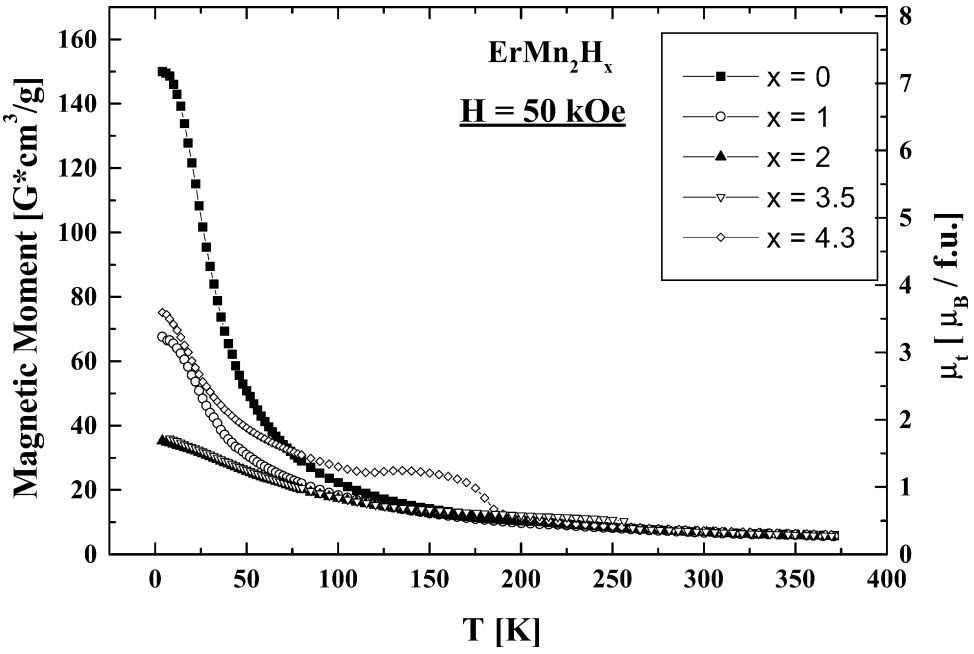

Fig. 7. Magnetisation in function of temperature for $ErMn_2H_x$ hydrides taken at 50 kOe (5 T).

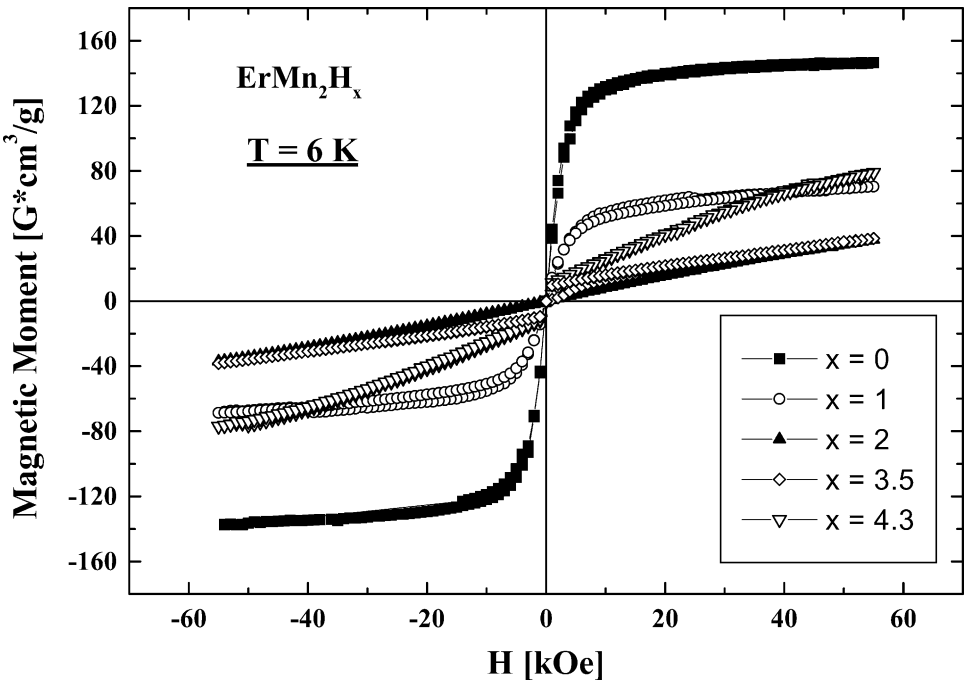

Fig. 8. The field dependencies of the $ErMn_2H_x$ magnetisation at 6 K.

380 K, already. The complicated magnetic behaviour of the $ErMn_2H_{4.3}$ sample consisting of several phases can be judged from the field dependence of the magnetic susceptibility shown in Fig. 9. In the temperature range of a rather weak volume, anomaly of both phases around 200 K (Fig. 2) at least two magnetic anomalies can be discerned in Fig. 9. Whereas the magnetic susceptibility is rather temperature independent in the 50–100 K range, two anomalies follow for higher temperatures. A maximum of the susceptibility at about 150–160 K is followed by a rather abrupt decrease of the susceptibility at about 180 K that is clearly visible even in the highest field data. On the other hand, a second step-like susceptibility decrease for increasing temperature at about 225 K can be best observed in the low-field data. However, such data for multiphase hydrides are not usable for a more detailed quantitative analysis.

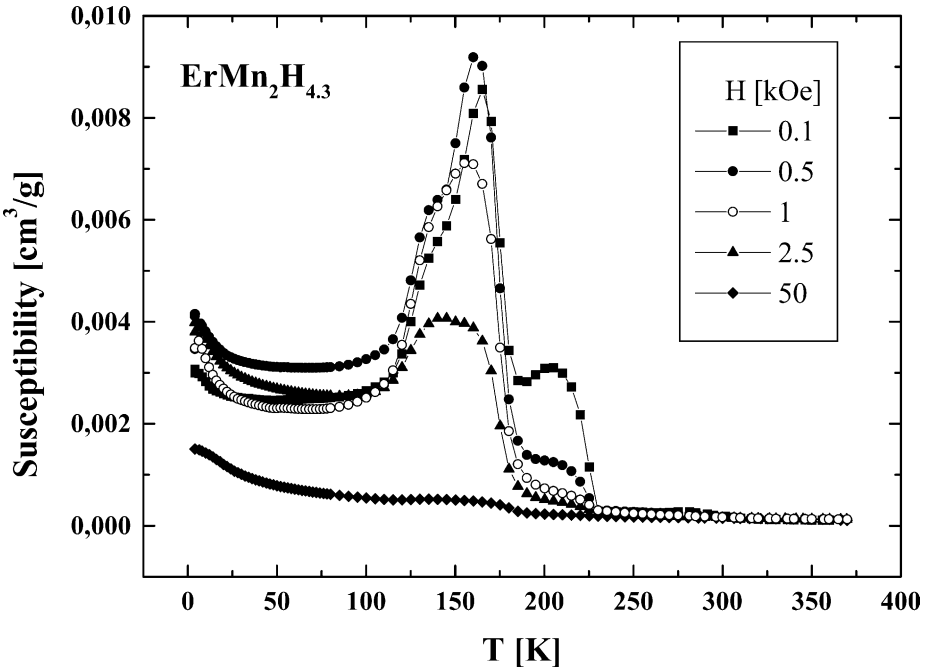

Fig. 9. The temperature dependencies of the susceptibility for $ErMn_2H_{4.3}$ taken at different conditions.

5. Conclusions

For the hexagonal hydrides $ErMn_2H_x$ ($0 < x < 4.3$) in a similar way as for the cubic Laves phase hydrides, we observe the structural transformations, and in particular a temperature dependent phase decomposition of spinodal type for some hydrogen concentration ranges. However, for $ErMn_2H_1$ an onset of spinodal decomposition takes place at higher temperature than for the cubic hydrides, which on the one hand suggest its dependence on the rare earth atom, on the other hand relates it with the structure (cubic or hexagonal), which in fact is also connected with the rare earth atoms. For $ErMn_2H_3$, a spinodal decomposition into two phases with slightly differing hydrogen content is observed, similarly as for $SmMn_2H_2$, but for higher concentration of hydrogen.

Another interesting effect is in the clear distortions for the single-phase hydrides ($x = 2$; 3.5) accompanying the onset of magnetic order, not visible for the cubic hydrides besides of YMn_2 [1].

The temperature dependent magnetic anomalies of the $ErMn_2H_x$ samples are richer in details than for the cubic rare earth hydrides studied before and partially rather pronounced, most prominent in the low field measurements. Of all the $ErMn_2H_x$ hydrides studied in the current investigation, the dihydride is the compound with the weakest magnetization in its magnetically ordered state below 205 K even in external magnetic fields of 55 kOe. Evidently, the strength of the collinear coupling between the Er sublattice(s) and the antiferromagnetically coupled Mn sublattices is especially large for this compound.

References

[1] H. Figiel, J. Przewoźnik, V. Paul-Boncour, A. Lindbaum, E. Gratz, M. Latroche, M. Escorne, A. Percheron-Guégan, P. Mietniowski, J. Alloys Compd. 274 (1998) 29.
[2] J. Przewoźnik, J. Żukrowski, K. Freindl, E. Japa, K. Krop, J. Alloys Compd. 284 (1999) 31.
[3] H. Figiel, A. Budziak, J. Żukrowski, G. Fischer, M.T. Kelemen, E. Dormann, J. Alloys Compd. 335 (2002) 48.
[4] J. Żukrowski, H. Figiel, A. Budziak, P. Zachariasz, G. Fischer, E. Dormann, J. Magn. Magn. Mat. 238 (2002) 129.
[5] I.N. Goncharenko, I. Mirebeau, A.V. Irodova, E. Suard, Phys. Rev. B. 59 (1999) 9324.
[6] H. Figiel, A. Budziak, J. Żukrowski, Solid State Commun. 111 (1999) 519.
[7] H. Figiel, Cz. Kapusta, A. Budziak, P.C. Riedi, J. Alloys Compd. 330–332 (2002) 361.
[8] Y. Makichara, Y. Andoh, Y. Hasimoto, H. Fuji, M. Hasuo, T. Okamoto, J. Phys. Soc. Jpn. 52 (1983) 629.
[9] S. Labroo, N. Ali, J. Appl. Phys. 67 (1990) 5292.
[10] H. Wada, H. Nakamura, K. Yoshimura, M. Shiga, Y. Nakamura, J. Magn. Magn. Mat. 70 (2001) 134.
[11] J. Rodriguez-Carvajal, Abstract Satellite Meeting on Powder Diffraction of the 15th Congress of the International Union of Crystallography, Toulouse, France, 1990, p. 127.
[12] P.W. Sellwood, in: Magnetochemistry, Interscience, New York, 1956, p. 78.
[13] E. Burzo, A. Chełkowski, H.R. Kirchmayr, in: H.P.J. Wijn (Ed.), Landolt-Börnstein Numerical Data..., vol. 19, subvol. d2, Springer-Verlag, 1990, p. 86, Table 38a.
[14] H. Figiel, A. Budziak, J. Żukrowski, Solid State Commun. 111 (1999) 519.
[15] P.J. Viccario, G.K. Shenoy, D. Niarchos, B.D. Dunlap, J. Less-Common Met. 73 (1980) 265.
[16] H. Figiel, A. Budziak, B. Ouladdiaf, G. Wiesinger, Neutron diffraction study for $ErMn_2D_2$, ILL Grenoble, 2002, unpublished results.